the FEBS Journal

A di-leucine sorting signal in ZIP1 (SLC39A1) mediates endocytosis of the protein

Liping Huang[1,2] and Catherine P. Kirschke[1]

1 United States Department of Agriculture/Agriculture Research Service/Western Human Nutrition Research Center, Davis, CA, USA
2 Department of Nutrition and Rowe Program in Genetics, University of California at Davis, CA, USA

Keywords
di-leucine; endocytosis; Golgi apparatus; SLC39; zinc transporters

Correspondence
L. Huang, 430 West Health Sciences Drive, Davis, CA 95616, USA
Fax: +1 530 752 5295
Tel: +1 530 754 5756
E-mail: lhuang@whnrc.usda.gov

(Received 9 April 2007, revised 31 May 2007, accepted 11 June 2007)

doi:10.1111/j.1742-4658.2007.05933.x

It has been demonstrated that the plasma membrane expression of ZIP1 is regulated by endocytic mechanisms. In the zinc-replete condition, the level of surface expressed ZIP1 is low due to the rapid internalization of ZIP1. The present study aimed to identify a sorting signal(s) in ZIP1 that mediated endocytosis of ZIP1. Four potential sorting signals (three di-leucine- and one tyrosine-based) were found by searching the eukaryotic linear motif resource for functional sites in proteins (http://elm.eu.org). Site-directed mutagenesis and immunofluorescence microscopic analyses demonstrated that the di-leucine sorting signal, ETRALL144–149, located in the variable loop region of ZIP1, was required for the ZIP1 internalization and lysosomal degradation. Substitutions of alanines for the di-leucine residues (LL148,149/AA) severely impaired the internalization of ZIP1 and subsequent protein degradation, leading to an accumulation of the mutant ZIP1 on the cell surface, as well as inside the cell. Using chimeric proteins composed of an α-chain of interleukin-2 receptor fused to the peptides derived from the variable loop region of ZIP1, we found that the di-leucine sorting signal of ZIP1 was required and sufficient for endocytosis of the chimeric proteins.

Intracellular zinc homeostasis is achieved through coordinated regulations of different zinc transporters involved in influx, efflux, and intracellular compartmental sequestration or release. Two families of zinc transporters (SLC30, ZNT and SLC39, ZIP) have been identified in mammals [1–18]. The ZIP members are essential for an increase of cytoplasmic zinc concentrations by enhancement of zinc uptake or release of the stored zinc from subcellular compartments to the cytoplasm of the cell when zinc is deficient [18]. On the other hand, zinc efflux and intracellular compartmentation are accomplished by the members of the ZNT proteins when zinc is in excess [9].

The ZIP proteins (SLC39A1-14) are predicted to have eight transmembrane domains with an intracellular cytosolic histidine-rich loop (variable loop region) between transmembrane domains III and IV [19]. They share little conservation both in the sequence and the length of the loop in this region, except for the sequence $(HX)_n$ where H is the histidine residue, X is usually aspartic acid, glutamic acid, glycine, lysine, asparagines, arginine, or serine, and *n* generally is in the range 2–5 [18]. The histidine residues in the loop region of ZIP proteins are thought to bind zinc. However, the exact function of the loop region is not understood.

Regulations of the ZIP protein activities have been found to occur at multiple levels, including transcription [20–23] and intracellular protein trafficking [14,24,25]. Intracellular trafficking of ZIP1, ZIP3, ZIP4, and ZIP5 appears to be a regulated process important for maintaining cellular zinc homeostasis [14,24,25]. In zinc-depleted cells, ZIP proteins seem to be internalized more slowly from the plasma

Abbreviations
CHO, Chinese hamster ovary; EST, expressed sequence tag; IL2RA, α-chain of interleukin-2 receptor; TfR, transferrin receptor; TGN, *trans* Golgi network; ZIP, ZRT, IRT-like protein family; ZNT, zinc transporter.

membrane, resulting in an accumulation of the activated ZIP proteins on the cell surface, which leads to an increased zinc influx. On the other hand, in zinc-replete cells, these ZIP proteins are rapidly removed from the plasma membrane to intracellular compartments. The internalization of ZIP proteins from the cell surface lowers the amount of proteins available for zinc uptake on the cell surface, which leads to a decrease in zinc influx [24,26]. Endocytosis, recycling, and/or degradation of ZIP proteins contribute to the rapid modulation of the amount of surface zinc uptake proteins in response to the change in cellular zinc concentrations. By changing the relative rate of zinc uptake protein internalization, cells can adjust the intracellular labile zinc pool level promptly.

Many plasma membrane proteins bear their endocytic signals within the cytosolic domains of proteins. These signals, identified by sequence correlations and mutational analyses, are a short stretch of consensus amino acid residues with key residues for their function. These signals are thought to interact with specific recognition molecules to form transport intermediates that sort membrane proteins into different sites within cells [27]. The best understood endocytic signals are the di-leucine ([DER]XXXL[LVI]) and tyrosine-based sorting signals. The di-leucine signals with consensus sequences [DE]XXXL[LI] predominantly target membrane proteins from the cell surface to the endosomal–lysosomal compartments [27]. Most tyrosine-based signals conform to the consensus sequences YXXØ, where X is any amino acid and Ø is an amino acid with a bulky hydrophobic side chain. The tyrosine-based signal is responsible for endocytosis of membrane proteins and direct sorting of membrane proteins to a variety of intracellular compartments [28]. Both [DE]XXXL[LI] and YXXØ can be recognized by heterotetrameric adaptor protein complexes (AP-1, AP-2, and AP-3) with a distinct affinity of interaction in the formation of clathrin–AP coat complexes [27,29,30]. The YXXØ signal can also be recognized by a fourth AP complex (AP-4) for protein sorting [31,32].

The cellular localization of zinc transporters including ZIP1, ZIP3–5, ZNT4, and ZNT6 are regulated in response to the fluctuations of cellular zinc concentrations [6,14,24,25,33]. However, the sorting signals for the intracellular protein trafficking carrying in these transporter proteins are not clear. The present study aimed to identify a sorting signal(s) in ZIP1 that mediated the internalization of ZIP1. Here, we demonstrate that a stretch of six amino acids with a consensus sequence for a di-leucine signal (EXXXLL144–149) in the variable loop region of ZIP1 plays a critical role in mediating ZIP1 endocytosis and protein degradation. We further demonstrate that this internalization signal of ZIP1 is sufficient for the endocytosis of the IL2R-ZIP1 chimeric proteins.

Results

Identification of an endocytic signal(s) in ZIP1

ZIP1 resides intracellularly when cellular zinc is adequate. However, when the cellular zinc concentration decreases, ZIP1 moves from its intracellular compartments towards the plasma membrane where it transports zinc into the cytoplasm. Targeting of plasma membrane proteins to intracellular compartments is largely dependent upon sorting signals contained within cytosolic domains of the proteins [34]. Therefore, we hypothesized that a sorting signal(s) in the cytosolic domains of ZIP1 may serve as a signal for the internalization of ZIP1. The potential sorting signal(s) in ZIP1 were first sought by examining the functional sites predicted in ZIP1 using the ELM server (the eukaryotic linear motif resource for functional sites in proteins; http://elm.eu.org). Both di-leucine (amino acids 6–11, 144–149, and 179–184) and tyrosine-based (amino acids 285–288) sorting signals were found in ZIP1 by the search (Fig. 1A). The di-leucine signal at amino acids 179–184 and the tyrosine-based signal at amino acids 285–288 are located within the predicted transmembrane domains that make them unlikely to be the signals for protein internalization (Fig. 1B) [27].

Localization of the wild-type (wt) and mutant ZIP1-Myc proteins in Chinese hamster ovary (CHO) cells

We introduced nonconservative amino acids (alanines) to replace the key amino acids in these potential ZIP1 endocytic signals to analyze their roles in the endocytosis of ZIP1. Expression plasmids containing cDNAs that encoded for either the wt or mutant ZIP1 proteins tagged with a Myc epitope at the C-terminal end of the proteins were transfected into CHO cells. Individual clones were selected and evaluated for the expression of mRNA of the wt and mutant ZIP1-Myc by real-time quantitative RT-PCR assays (data not shown). Clones expressing comparative amount of the wt or mutant ZIP1-Myc mRNA were chosen for use in this study.

Previous studies from our laboratory and others have demonstrated that both the endogenous ZIP1 and the epitope tagged ZIP1 (either the N- or C-terminal

A

Elm Name	Consensus sequence	Matched amino acid sequence in ZIP1	Position	Mutated motif
TRG_LysEnd_APsAcLL_1	[DER]...L[LVI]	EPELLV	6-11	EPEAAV
		ETRALL	144-149	ETRAAA
		RACVLV	179-184	RACAAV
TRG_ENDOCYTIC_2	Y..[LMVIF]	YITF	285-288	AITF

B

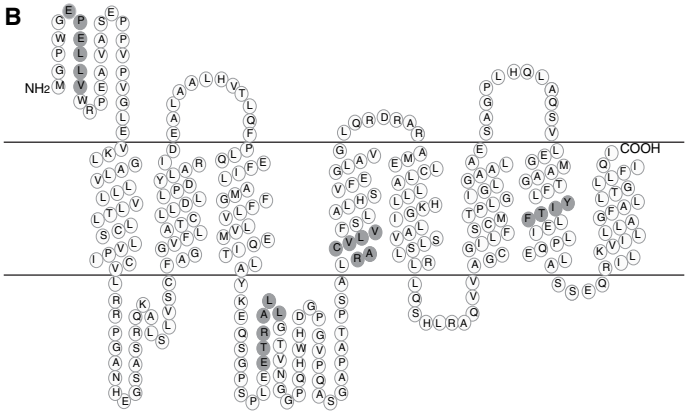

Fig. 1. Predicted sorting signals from human ZIP1. (A) List of predicted sorting signals. The indicated di-leucine and Y-based sorting signals in human ZIP1 were identified by searching the amino acid sequences of ZIP1 against the ELM resource. The ELM names and the consensus sequences for the predicted signals are given. The predicted di-leucine and YXXø signal sequences and locations in ZIP1 are also given. The corresponding mutated signal sequences in ZIP1 are listed. (B) Schematic representation of the amino acid sequences and topologic structure of ZIP1. The topologic structure was determined by the SOSUI system (http://sosui.proteome.bio.tuat.ac.jp). The space between lines indicates the cell membrane. The predicted di-leucine and YXXø sorting signals are indicated as dark gray circles.

tagging) proteins predominantly reside within the cell in many adhesively cultured cells in the zinc-replete condition [24,35,36]. Therefore, we predicted that the wt ZIP1-Myc protein, when stably expressed in CHO cells, would be predominantly localized in intracellular compartments in normal culture conditions. As shown in Fig. 2, the wt ZIP1-Myc protein was mostly detected in the perinuclear region of the CHO cells with a punctate distribution in the cytoplasm of the cell (Fig. 2A). The perinuclear staining of the wt ZIP1-Myc protein was strikingly coincident with the Golgi marker GM130 [37] determined by the double immunofluorescence microscopic assay (Fig. 2A–C) and was sensitive to the treatment of brefeldin A, a fungal macrocyclic lactone known to specifically disrupt the Golgi apparatus of the cell (data not shown) [6,7]. Moreover, when the ZIP1-Myc protein was costained with the trasferrin receptor (TfR), a plasma membrane protein that recycles to the *trans* Golgi network shortly after internalization via recycling endosomes [38], the overlapping staining was only detected in the perinuclear region of the cell (Fig. 2F). The vesicular staining

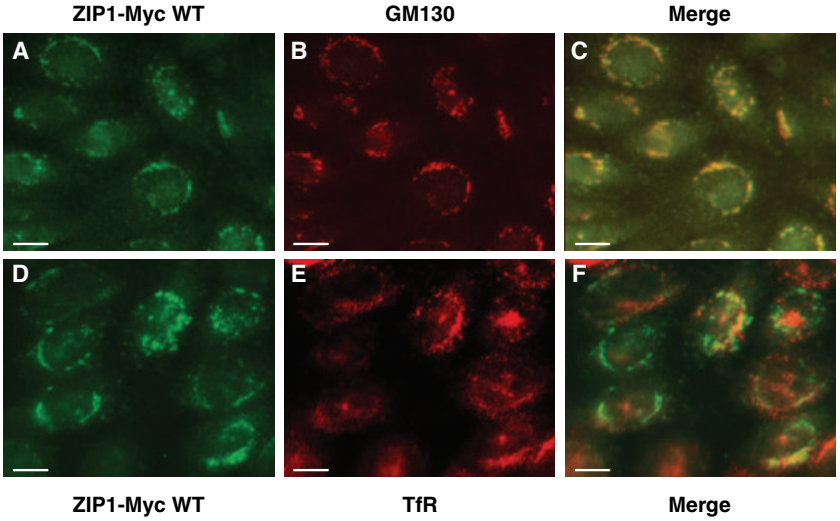

Fig. 2. Localization of the wt ZIP1-Myc, GM130 or TfR protein in CHO cells. CHO cells stably expressing the wt ZIP1-Myc protein were grown in slide chambers. Cells were washed, fixed, permeabilized, and double-stained with a rat Myc antibody (A,D) and a mouse GM130 antibody (B) or a mouse TfR (E) antibody followed by Alexa 488-conjugated goat anti-rat serum (green) or Alexa 594-conjugated goat anti-mouse serum (red). Yellow staining in (C) and (F) indicates the overlapping expression of ZIP1-Myc with GM130 or TfR in CHO cells. Scale bars = 10 μM.

patterns were distinctive between ZIP1-Myc and TfR (Fig. 2D–F). Taken together, these results strongly suggest that the wt ZIP1-Myc protein is associated with the Golgi apparatus and an intracellular vesicular compartment that distinguishes from the recycling vesicles containing TfR in CHO cells.

Having demonstrated the cellular localization of the wt ZIP1-Myc protein in the Golgi apparatus, as well as in an intracellular vesicular compartment of CHO cells, we then compared the distribution of the mutant ZIP1-Myc proteins in CHO cells with the wt ZIP1-Myc protein. No noticeable differences in the intracellular distribution between the wt ZIP1-Myc and mutant ZIP1-Myc proteins that carried the mutations at amino acids 9–10 (LL/AA), 182–183 (VL/AA), or 285 (Y/A) were observed (Fig. 3A,B,D,E). However, the mutant ZIP1-Myc protein that carried mutations at amino acids 148–149 (LL/AA), which disrupted a predicted di-leucine signal, exhibited a diffused staining pattern that implied the cell surface distribution (Fig. 3C).

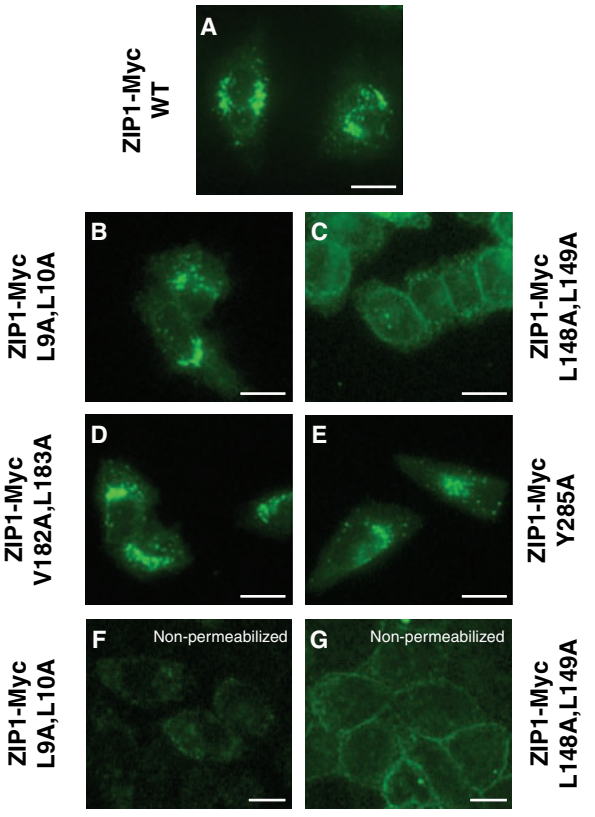

Fig. 3. Effect of site-directed mutations on the intracellular localization of ZIP1-Myc in CHO cells. Stably transfected CHO cells were grown in slide chambers. Cells were washed, fixed, and permeabilized before immunofluorescent staining (A–E). Where indicated, cells were washed and fixed but not permeabilized before immunofluorescent staining (F,G). The wt and mutant ZIP1-Myc proteins were detected by a mouse Myc antibody (4 $\mu g \cdot mL^{-1}$) followed by an Alexa 488-conjugated goat anti-mouse serum (1 : 500 dilution). Scale bars = 10 μM.

To examine whether the diffused staining pattern observed in CHO cells expressing the mutant (L148A,L149A) ZIP1-Myc protein was caused by an accumulation of the mutant protein on the cell surface, we performed an indirect immunofluourscence microscopic assay. In this assay, cells were fixed but not permeabilized, permitting the detection of cell surface expressed ZIP-Myc only. The C-terminal tagged Myc epitope in ZIP1 is predicted to be extracellular and therefore allowed Myc antibody binding in nonpermeabilized cells [24]. As shown in Fig. 3F, weak membrane staining was observed in the CHO cells expressing the wt ZIP1-Myc protein. In contrast, a much stronger cell surface staining was detected in the CHO cells expressing the mutant ZIP1-Myc protein (L148A,L149A) (Fig. 3G).

The increased level of the mutant (L148A,L149A) ZIP1-Myc protein expressed on the cell surface of CHO cells was further confirmed by western blot analyses with a total of six independent CHO cell lines expressing either the wt ZIP1-Myc (three cell lines) or the mutant ZIP1-Myc protein (three cell lines) (Fig. 4). Multiple independent cell lines that expressed comparable amount of the wt or mutant ZIP1-Myc mRNA were included in this assay to eliminate errors introduced by using single cell line. In this assay, cells were fixed and blocked. The surface expressed ZIP1-Myc proteins (wt or mutant) were then bound by mouse Myc antibodies. The unbound antibodies were removed by extensive washes. Proteins including Myc antibodies were separated on Tris-HCL gels and transferred to nitrocellulose membranes. Myc antibodies, representing the surface expression levels of ZIP1-Myc (wt or mutant), were then detected by a peroxidase-conjugated secondary antibody, quantified by densitometry, and normalized by the expression of an endoplasmic reticulum house keeping protein, GRP78 (Fig. 4A). The quantitative data indicated that the mean surface expression level of the mutant ZIP1-Myc protein was 2.3-fold higher than that of the wt ZIP1-Myc protein (Fig. 4B). Taken together, these results suggest that the wt ZIP1-Myc protein exhibits a steady-state localization in the Golgi apparatus and an unknown vesicle compartment in the stably transfected CHO cells and the disruption of a di-leucine signal in the variable loop region of ZIP1 increased cell surface expression of ZIP1.

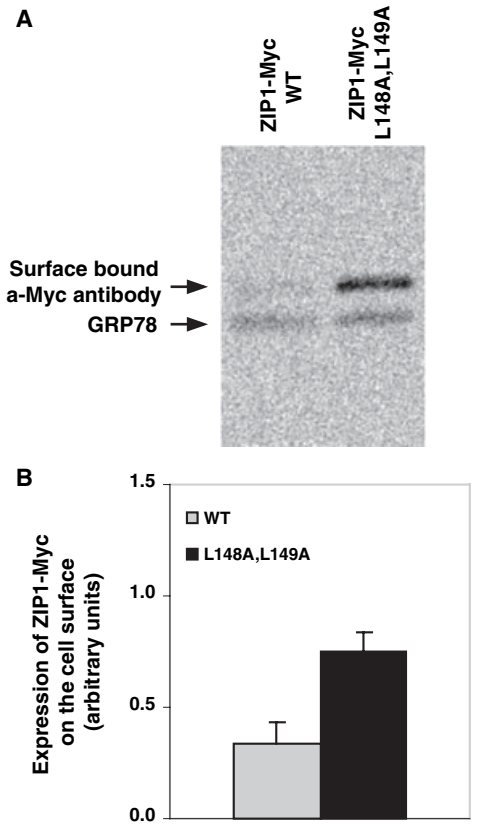

Fig. 4. Expression of the wild-type and mutant (L148A,L149A) ZIP1-Myc proteins on the surface of CHO cells. Stably transfected CHO cells expressing either the wt ZIP1-Myc or the mutant (L148A,L149A) ZIP1-Myc protein were cultured in six-well plates. Lysate containing bound Myc antibodies was prepared as described in the Experimental procedures. (A) A representative western blot analysis. Western blot containing 50 μg of protein extracts was probed with a peroxidase-conjugated goat anti-mouse serum. The protein bands were visualized using a Super Signal west femto kit (Pierce). The GRP78 expression level on the same western blot was served as loading control. (B) Quantification of the expression levels of the wt and mutant ZIP1-Myc proteins on the cell surface. Western blot analysis (A) was performed with the cell lysate isolated from six individual stably transfected CHO cell lines either expressing the wt ZIP1-Myc (three cell lines) or mutant ZIP1-Myc protein (three cell lines). The signals from these western blots were quantified by an Alpha Innotech Gel Documentation System. The expression of either the wt or mutant ZIP1-Myc protein was then normalized by the expression of GRP78. Values are the means ± SE ($n = 3$).

Mutation of the endocytic di-leucine signal ($LL_{148,149}$) of ZIP1 decreased internalization of the protein

To directly measure the effects of mutations in the di-leucine signal of ZIP1 on internalization, an immuno-endocytosis assay was performed. In this experiment, cells expressing the wt or mutant (L148A,L149A) ZIP1-Myc protein were incubated with Myc antibodies at 37 °C for 1 h to allow ZIP1-Myc/Myc antibody complexes to be internalized. Both surface bound Myc antibodies and those that had been internalized, which were revealed by extensive washes with an acid buffer to remove surface bound antibodies, were detected with an Alexa 488-conjugated goat anti-mouse secondary serum by immunofluorescence microscopy analyses. To ensure that any decrease in internalization was not simply caused by the decreased endocytic efficiency due to the overexpression of the ZIP1-Myc proteins in CHO cells, the internalization of TfR was also examined in the cells expressing the wt or mutant ZIP1-Myc protein by immunofluorescence microscopy analyses. As shown in Fig. 5, wt ZIP1-Myc bound Myc antibodies were internalized efficiently (Fig. 5B), comparable to that of TfR bound antibodies (Fig. 5D). However, no significant amount of the internalized mutant ZIP1-Myc protein bound Myc antibodies were detected in CHO cells (Fig. 5F). In contrast, most TfR bound antibodies on the surface of these cells were internalized after 1 h of incubation (Fig. 5H), indicating that the endocytic machinery in these mutant ZIP1-Myc expressing cells was intact. Taken together, these results suggest that the reduction in the internalization of the mutant ZIP1-Myc protein from the cell surface resulted from the mutations in the di-leucine trafficking signal, $ETRALL_{144–149}$, of ZIP1.

Internalization of ZIP1 from the cell surface is important for the degradation of ZIP1-Myc

The di-leucine signals with [DE]XXXL[LI] consensus sequences mediates rapid internalization of plasma proteins and delivers them to the endosomal–lysosomal compartment where proteins are subjected to degradation [39–43]. To determine whether or not substitutions of the di-alanine residues for the di-leucine residues ($LL_{148,149}$) have an effect on degradation of ZIP1, we compared the total protein expression levels of the wt ZIP1-Myc protein with that of the mutant (L148A,L149A) ZIP1-Myc protein in a total of six independent CHO cell lines expressing either the wt ZIP1-Myc (three cell lines) or the mutant (L148A,L149A) ZIP1-Myc protein (three cell lines) by western blot analyses. As shown in Fig. 6A,B, the total expression of the mutant ZIP1-Myc protein in CHO cells was 3.6-fold higher than that of the wt ZIP1-Myc protein. Given that the $LL_{148,149}$/AA mutations increased the cell surface expression of the mutant ZIP1 protein by approximately 2.3-fold (Fig. 4B), additional accumulation of the mutant ZIP1 protein

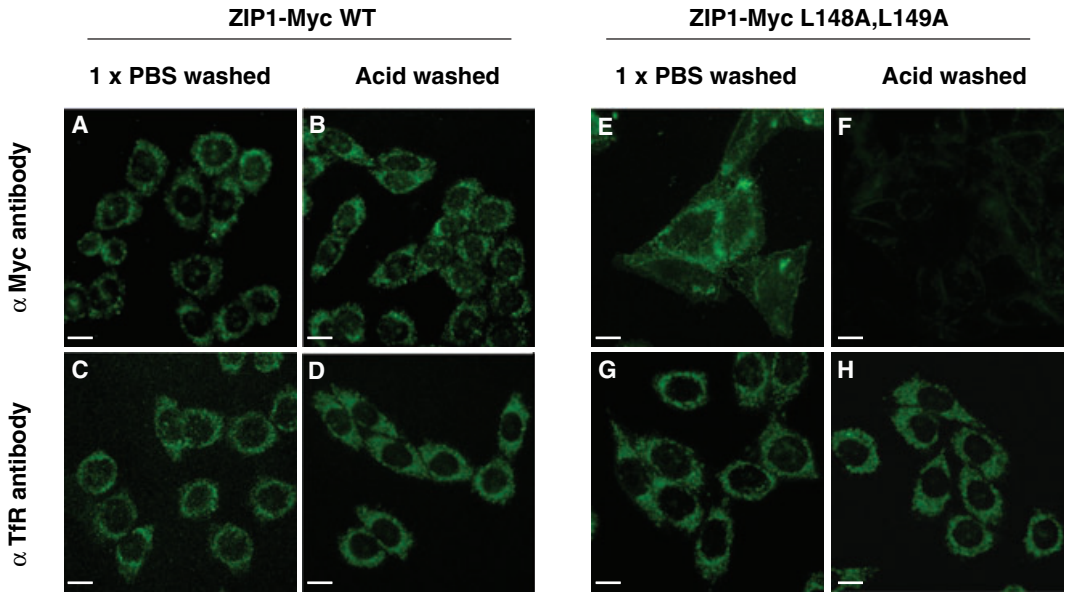

Fig. 5. Internalization of the wild-type or mutant (L148A,L149A) ZIP1-Myc protein in the stably transfected CHO cells. Cells were cultured in slide chambers for 24 h and then incubated with either a mouse Myc (20 μg·mL^{-1}) or a mouse TfR (5 μg·mL^{-1}) antibody for 1 h. Surface bound Myc or TfR antibodies were removed by washing with ice-cold acidic buffer (B,D,F,H) [24]. The control cells were washed with ice-cold 1 × NaCl/Pi (A,C,E,G). Cells were then fixed and permeabilized. The internalized Myc or TfR antibodies were detected by an Alexa 488-conjugated goat secondary antibody (1 : 250 dilution). Scale bars = 10 μM.

inside the CHO cells suggests that the ETRALL$_{144–149}$ sorting signal of ZIP1 may also play a role in signaling of the protein for degradation.

To confirm the involvement of the lysosome in degradation of ZIP1-Myc, we determined the effects of cycloheximide, an inhibitor of protein biosynthesis in eukaryotic cells, and chloroquine, a lysosomal degradation inhibitor [43], on the accumulation of the wt and mutant ZIP-Myc proteins in the stably transfected CHO cells. As shown in Fig. 6C,D, incubation of cells with cycloheximide decreased the total expression levels of either the wt or mutant ZIP1-Myc proteins in the cells. However, treatment of cells with cycloheximide did not change the expression ratio between the wt and mutant ZIP1-Myc proteins. In contrast, in the presence of chloroquine, the total ZIP1-Myc accumulation in the CHO cells expressing the wt ZIP1-Myc protein was increased to the level that was detected in the cells expressing the mutant ZIP1-Myc protein, indicating that the wt ZIP1-Myc protein was preferentially degraded by the lysosomal pathway and the di-leucine signal was required for this process.

Expression of chimeric proteins

To confirm that the loop region sequence of ZIP1 is sufficient and independent as the endocytic sorting signal, we generated two constructs in which the wt and mutant ZIP1 (L148A,L149A) loop region sequences (amino acids 133–177) (Fig. 1B) were fused to the C-termini of the ectoplasmic and transmembrane domains of interleukin-2 receptor-α (Fig. 7A) and expressed as IL2R/ZIP1_C1 and IL2RA/ZIP1_C5 chimeric proteins, respectively, in CHO cells. The subcellular localization of IL2RA/ZIP1_C1 and IL2R/ZIP1_C5 was detected by a IL2RA antibody followed by an Alexa 488-conjugated goat secondary antibody. As shown in Fig. 7B, the IL2RA-ZIP1 chimera with the wt ZIP1 loop region sequence (IL2RA/ZIP1_C1) was detected predominantly in the perinuclear region of the cell (Fig. 7C) with limited amount on the cell surface (Fig. 7D) whereas the IL2RA protein alone was found largely on the cell surface (Fig. 7A,B). In contrast, the subcellular localization of the IL2RA-ZIP1 chimera with the mutant ZIP1 loop region sequence (IL2RA/ZIP1_C5) was found predominantly on the plasma membrane (Fig. 7E,F). Furthermore, deletions of the amino acids adjacent to the di-leucine signal (IL2RA/ZIP1_C2, IL2RA/ZIP1_C3, and IL2RA/ZIP1_C4) (Fig. 7A) did not affect the efficiency of the internalization of the IL2RA/ZIP1 chimeric proteins (Fig. 7G–I).

The cellular localization of IL2RA/ZIP1_C1 and IL2RA/ZIP1_C5 chimera is similar to the wt

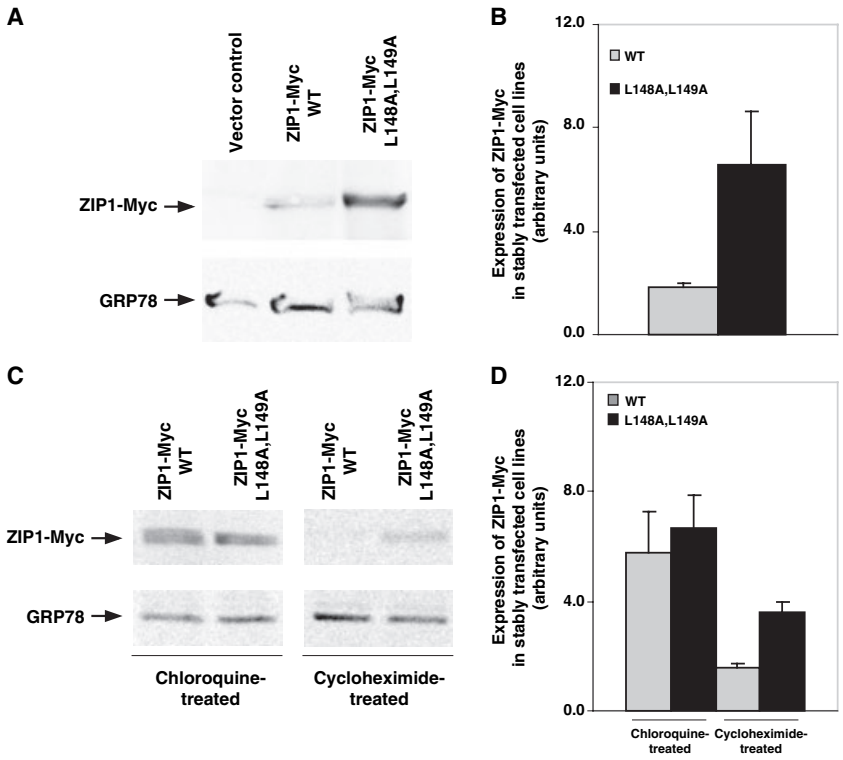

Fig. 6. Effect of mutations (L148A,L149A) in ZIP1 on the total protein expression and protein degradation in CHO cells. (A) Western blot analysis of total ZIP1-Myc protein accumulation in CHO cells. Stably transfected CHO cells expressing the vector control, wt, or mutant ZIP1-Myc protein were harvested and lysed. Proteins (50 μg) were separated by SDS/PAGE and transferred to a nitrocellulose membrane. The blot was probed with a Myc antibody (2 $\mu g \cdot mL^{-1}$) followed by a peroxidase-conjugated goat secondary antibody (1 : 2500 dilution). The same blot was sequentially probed with a GRP78 antibody (4 $ng \cdot mL^{-1}$) followed by a peroxidase-conjugated goat secondary antibody (1 : 10 000 dilution) for the loading control. (B) Quantification of the expression levels of the wt and mutant ZIP1-Myc proteins. Western blot analysis (A) was performed with the cell lysate isolated from six individual stably transfected CHO cell lines either expressing the wt (three cell lines) or mutant (three cell lines) ZIP1-Myc protein. The wt ZIP-Myc, mutant ZIP1-Myc, and GRP78 protein bands from these western blots (a representative western blot is shown in A) were quantified by an Alpha Innotech Gel Documentation System. The expression of either the wt or mutant ZIP1-Myc protein was normalized by the expression of GRP78. Values are the means ± SE, $n = 3$. (C) Effects of cycloheximide and chloroquine on the accumulation of the wt or mutant ZIP1-Myc protein in CHO cells. Cells were treated with either cycloheximide (10 $\mu g \cdot mL^{-1}$) or chloroquine (0.2 mM) at 37 °C for 3 h before harvest. Protein lysate (50 μg) was separated by SDS/PAGE and transferred to a nitrocellulose membrane. The western blot analyses were performed as described in (A). (D) Quantification of the expression levels of the wt or mutant ZIP1-Myc protein in either cycloheximide- or chloroquine-treated CHO cells. The densitometric analysis of the protein bands on the western blots (a representative western blot shown is in C) was performed as described in (B).

ZIP1-Myc and mutant (L148A,L149A) ZIP1-Myc proteins in CHO cells, respectively (Fig. 3A,C), suggesting that the IL2RA/ZIP1_C1 fusion protein was internalized efficiently from the plasma membrane into the cytoplasmic compartment by the di-leucine signal of ZIP1 and substitutions of the di-alanine residues for the di-leucine residues in the ZIP1 sorting signal inhibited the internalization of the chimeric protein.

Discussion

It has been demonstrated that the extent of intracellular trafficking of ZIP through exocytosis and endocytosis is cell dependent [10,24,35]. Intracellular zinc deficiency reduces the endocytic arm. This facilitates uptake of zinc and restores normal cellular zinc homeostasis. On the other hand, when cellular zinc levels are elevated, the rate of endocytosis of ZIP1 is increased to reduce zinc influx. Previous studies have demonstrated that ZIP1 is constitutively endocytosed from the cell surface and travels to the intracellular compartments in the zinc-adequate condition [24]. In the present study, four potential protein trafficking signals in ZIP1 were revealed by searching the eukaryotic linear motif resource for functional sites in proteins. We demonstrate that a di-leucine sorting signal, $ETRALL_{144-149}$, located in the variable loop region of ZIP1, which has the consensus sequences of a leucine

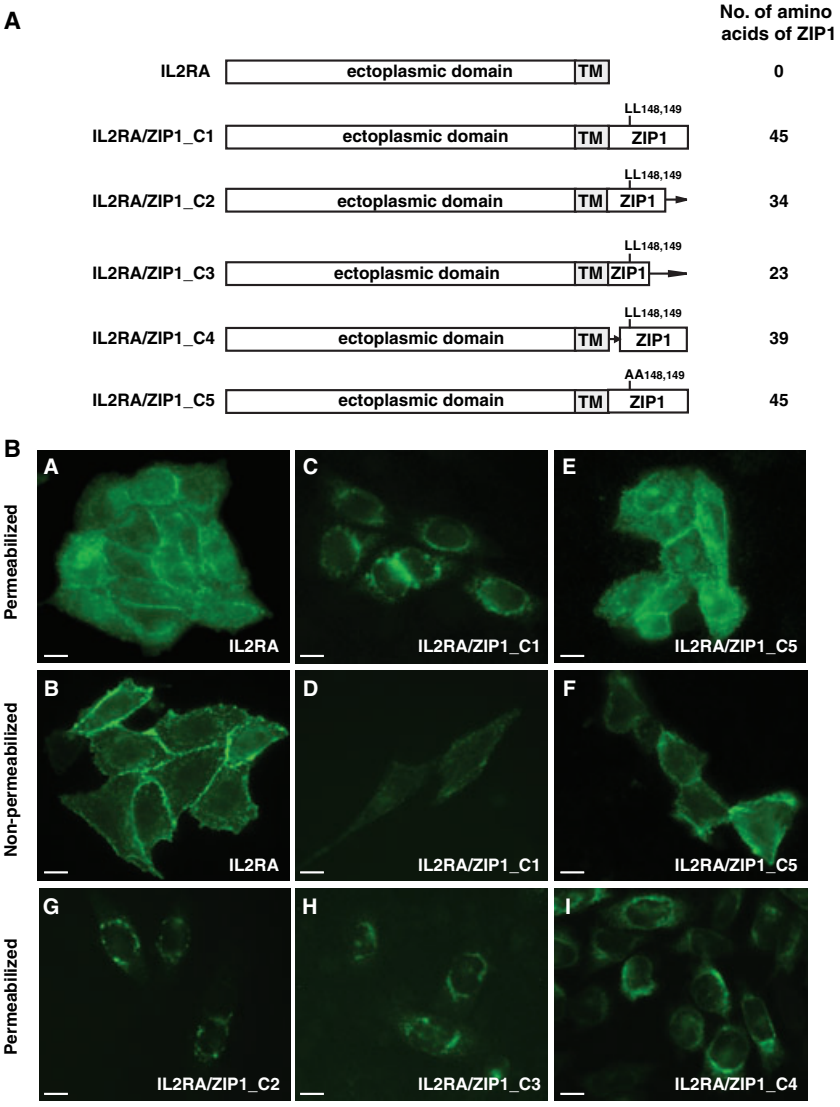

Fig. 7. Cellular localization of IL2RA and IL2RA-ZIP1 chimera. (A) Schematic representation of the IL2RA ectoplasmic and transmembrane domains and IL2RA/ZIP1 chimera. Forty-five amino acids of the loop region of ZIP1 were fused to the C-terminal end of the transmembrane domain of IL2RA (IL2RA/ZIP1_C1). Deletions of the loop region sequences of ZIP1 are shown by horizontal arrows. The critical di-leucine residues in the ETRALL$_{144–149}$ sorting signal are shown and amino acids converted to alanines are indicated as AA. The numbers of the amino acids derived from the loop region of ZIP1 fused to IL2RA are listed on the right. (B) Immunofluorescence analysis. Stably transfected CHO cells were grown in slide chambers for 48 h. Cells were washed, fixed, and permeabilized before immunofluorescent staining (A,C,E,G,H,I). Cells in (B), (D), and (F) were fixed but not permeabilized for cell surface protein staining. The IL2RA and IL2RA/ZIP1 fusion proteins were detected by a mouse IL2RA antibody (1.7 μg·mL^{-1}) followed by an Alexa 488-conjugated goat secondary antibody (1 : 500 dilution). Scale bars = 10 μM.

doublet and an acidic residue at position −4 relative to the first leucine of the leucine doublet, facilitates the endocytosis of ZIP1 and protein degradation. Targeted mutations of the di-leucine residues in this signal led to in an increase in ZIP1 expression on the cell surface. Meanwhile, the mutations of the di-leucine residues resulted in a higher accumulation of ZIP1 within the cell due to the reduction in the lysosomal degradation of ZIP1. The discovery of a trafficking signal in a highly variable region of ZIP1 suggests that members of the ZIP family may utilize different trafficking signals within the proteins for intracellular organelle targeting. Nevertheless, a similar sequence (ESPELL) is found in the corresponding loop region of ZIP4 among the 14 ZIP proteins, suggesting that ZIP4 may undergo a similar trafficking pathway as ZIP1. Moreover, both di-leucine signals in ZIP1 and ZIP4 have another acidic residue further amino-terminal to the EXXXLL motif that adds to the strength of the signal for adaptor protein targeting [27].

In cultured CHO cells, the steady-state distribution of ZIP1 favors the Golgi localization (Figs 2 and 3). Disruption of the di-leucine signal (LL$_{148,149}$) had a detrimental effect on the endocytosis of ZIP1 but not on the intracellular trafficking of ZIP1 from the Golgi location to the cell surface, indicating that the signal for the plasma membrane targeting of ZIP1 is distinguished from the signal for plasma membrane retrieval and protein degradation. The signal(s) mediating the ZIP1 exocytotic arm of trafficking remains to be mapped.

The [DE]XXXL[LI] signals in mammalian proteins mediate rapid internalization and targeting to endosomal–lysosomal compartments. The location of a

functional di-leucine signal in the histidine-rich loop region of ZIP1 may bear physiological significance because the histidine residues in this region have been long suspected to be bound to zinc and play a role in zinc transport. Given that the sequence $(HX)_2$ is only eight amino acids downstream of the di-leucine signal ($LL_{148,149}$) and this di-leucine signal is required for the endocytosis of ZIP1, we hypothesize that the $(HX)_2$ in the variable loop region of ZIP1 may function as a sensor for cellular zinc concentrations. The interaction of the adaptor complex bound to the di-leucine signal with zinc bound histidine residues in $(HX)_2$ may be important for regulating the endocytosis rate of ZIP1 and subsequently targeting it to the lysosomal compartment for degradation under the zinc-replete condition.

It appears that signal-based regulation of metal transporters is a universal regulatory mechanism for early responses for the change in cellular metal concentrations. In yeast, the high affinity zinc uptake protein (ZRT1) was rapidly internalized and degraded through an ubiquitin conjugation signal located in the variable loop region of ZRT1 when cells were exposed to high zinc concentrations [26,44]. In mammalian cells, studies have shown that the cellular localization of zinc uptake proteins, including ZIP1, ZIP3, ZIP4, and ZIP5, are regulated in response to the fluctuation of cytoplasmic zinc concentrations [14,24,33]. However, the signal(s) in these proteins that mediate the plasma membrane targeting and retrieval has not been revealed. Identification of a di-leucine signal within ZIP1 that mediated the protein internalization and degradation in the present study highlights a molecular basis for zinc-induced regulations of zinc transporter expression on the cell surface. A similar motif was previously identified in a copper transporter, ATP7A [45–48]. The di-leucine signal ($LL_{147–148}$) proximal to the C-terminal tail of ATP7A mediates the recycling ATP7A from the plasma membrane to the *trans* Golgi network (TGN) in nonpolarized cells in the steady-state condition. However, the same signal in ATP7A is also responsible for targeting ATP7A from the TGN to the basal–lateral membrane of polarized cells to facilitate efflux of copper from the cell in a copper elevated condition.

We have previously reported that the protein expression level of ZIP1 in human prostate epithelial cells were down-regulated by zinc [36]. This zinc-induced down-regulation of ZIP1 expression was not associated with the transcriptional activity of the *ZIP1* gene [36]. Di-leucine signal-mediated lysosomal targeting and subsequent protein degradation after internalization of the protein have been observed in plasma membrane proteins, including epidermal growth factor receptor [49], β-site APP cleaving enzyme [50], and CD3 gamma [51,52]. Our observations that disruption of a functional di-leucine signal in ZIP1 inhibited the endocytosis of ZIP1, resulting in an accumulation of ZIP1 on the cell surface as well as inside the cell (present study), imply that a significant population of ZIP1 travels through the plasma membrane en route to lysosomes for protein degradation when cellular zinc is elevated.

In summary, we have identified a di-leucine protein trafficking signal in the variable loop region of ZIP1. Substitution of alanines for the leucine doublets in this di-leucine signal inhibited the internalization of ZIP1 in CHO cells. Disruption of this endocytic signal also led to an accumulation of ZIP1 within CHO cells.

Experimental procedures

Plasmid construction

The coding sequences of human ZIP1 (BI820953) were inserted into the pcDNA3.1/Myc-His vector (Invitrogen, Carlsbad, CA, USA). The DNA fragment in which the Myc epitope was fused in frame to the C-terminal end of ZIP1 was isolated from the resulting plasmid and cloned into the pcDNA5/FRT vector (Invitrogen) to create the plasmid ZIP1-Myc. Mutant constructs, ZIP1-Myc(L9A,L10A), ZIP1-Myc(L148A,L149A), ZIP1-Myc(V182A,L183A), and ZIP1-Myc(Y285A), were generated by QuikChange® II XL site-directed mutagenesis kit (Stratagene, La Jolla, CA, USA).

The cDNA fragment of IL2RA (amino acids 1–262) was obtained by PCR amplification of an EST clone (BG536515). The DNA fragments containing the loop region sequence of ZIP1 (amino acids 133–177) with or without LL/AA mutations were obtained by PCR amplification of the plasmid ZIP1-Myc or ZIP1-Myc(L148A,L149A). Plasmids IL2RA/ZIP1_C1 and IL2RA/ZIP1_C5 were generated by ligating the DNA fragments containing sequences encoding IL2RA and ZIP1 loop peptides (with or without the LL/AA mutations) into the pcDNA5/FRT vector. Other plasmids IL2RA/ZIP1_C2, IL2RA/ZIP1_C3, and IL2RA/ZIP1_C4, containing sequences encoding amino acids 133–166, 133–155, and 139–177 of ZIP1, respectively, were also constructed (Fig. 7A). All constructs generated for the present study were confirmed by DNA sequencing.

Cell culture and generation of stable cell lines

CHO/FRT cells were maintained according to the manufacture instructions (Invitrogen). The expressing and control cell lines were generated by transfecting plasmids into

CHO/FRT cells along with pOG44 (Flp recombinase) using a lipofectAMINE plus kit (Invitrogen). The stable cell lines were selected and maintained in the culture media containing 0.5–0.6 mg·mL^{-1} of hygromycin B.

Antibodies

Mouse Myc, TfR, GM130, GRP78, IL2RA, and rat Myc antibodies were purchased from Stressgen (Ann Arbor, MI, USA), Zymed Laboratories (South San Francisco, CA, USA), BD Biosciences (San Diego, CA, USA), Upstate (Lake Placid, NY, USA), and Serotec (Oxford, UK), respectively. Alexa 488- and 594-conjugated goat anti-mouse or anti-rat sera were purchased from Molecular Probes (Carlsbad, CA, USA). Peroxidase-conjugated goat anti-mouse serum was purchased from Pierce (Rockford, IL, USA).

Immunofluorescence microscopy

CHO cells expressing either the wt or mutant ZIP1-Myc protein were cultured in slide chambers for 48 h and fixed first with 3% paraformaldehyde in PEM buffer (0.1 M Pipes, pH 6.5; 1.0 mM $MgCl_2$; 1.0 mM EGTA) for 2.5 min at room temperature (RT) and then with 3% paraformaldehyde in borate buffer (0.1 M sodium borate, pH 11; 1.0 mM $MgCl_2$) for 5 min at RT. Cells were permeabilized with 0.5% Triton X-100 in 1 × NaCl/Pi, pH 7.4 for 15 min and blocked with 3% BSA for 30 min. The wt or mutant ZIP1-Myc proteins were detected using a Myc antibody (1 : 500 dilution, 1 h at RT) followed by an Alexa 488-conjugated goat secondary antibody (1 : 500 dilution, 1 h at RT). In the costaining assays, the wt ZIP1-Myc protein was detected by a rat Myc antibody (1 : 100 dilution, 1 h at RT) followed by an Alexa 488-conjugated goat secondary antibody (1 : 250 dilution, 1 h at RT). GM130 and TfR were detected by a mouse GM130 (1 : 750 dilution) and a mouse TfR (1 : 250 dilution) antibody, respectively, at RT for 1 h followed by an Alexa 594-conjugated goat secondary antibody (1 : 500 dilution, 1 h at RT). For detection of the ZIP1-Myc proteins on the cell surface, the permeabilization step was omitted.

In the study of endocytosis, cells were preincubated with Myc or TfR antibodies in media without fetal bovine serum at 37 °C for 1 h. Cells were then washed, fixed, and permeabilized [24]. Internalized Myc or TfR antibodies were detected by an Alexa 488-conjugated goat secondary antibody.

Cellular localization of IL2RA alone or IL2RA/ZIP1 fusion proteins in CHO cells was detected by immunofluorescence microscopic analyses. For the detection of IL2RA or IL2RA/ZIP1 fusion proteins on the cell surface, the permeabilization step was omitted. Cells were stained with a mouse IL2RA antibody followed by an Alexa 488-conjugated goat secondary antibody.

Western blot analysis

For analysis of the total wt and mutant ZIP1-Myc proteins expressed in CHO cells, CHO cells expressing wt ZIP1-Myc, mutant (L148A,L149A) ZIP1-Myc, or vector control were cultured in six-well plates at 37 °C for 48 h. Cell lysate was prepared and western blot analysis was performed as previous described [6]. The ZIP1-Myc (wt or mutant) and GRP78 proteins were detected by a mouse Myc and a mouse GRP78 antibody, respectively, followed by a peroxidase-conjugated goat secondary antibody. For analysis of wt or mutant ZIP1-Myc on the cell surface, CHO cells expressing wt or mutant (L148A,L149A) ZIP1-Myc were cultured in six-well plates at 37 °C for 24 h. Cells were fixed with ice-cold 4% paraformaldehyde. Nonspecific binding was blocked by incubation of cells with 3% BSA. Cells were then incubated with Myc antibodies at RT for 1 h and washed with 1 × NaCl/Pi, pH 7.4, to remove unbound antibodies. Cell were harvested, lysed, and western blot was performed [6]. Surface bound Myc antibodies were detected by peroxidase-conjugated goat secondary antibody. The GRP78 protein on the same blot was detected by GRP78 antibody followed by a peroxidase-conjugated goat secondary antibody. To examine the effects of cycloheximide and chloroquine on the expression of ZIP1-Myc in CHO cells, CHO cells expressing wt ZIP1-Myc or mutant (L148A,L149A) ZIP1-Myc were cultured in six-well plates for 24 h. The cells were then incubated for 3 h at 37 °C in the presence of either cycloheximide (10 μg·mL^{-1}) or chloroquine (0.2 mM). After incubation, the cells were washed three times with cold 1 × NaCl/Pi, pH 7.4. Cells were harvested, lysed, and western blot analyses were performed as described above. The densities of protein bands on the blots were measured by FluorChem^{TM} 8000 Advanced Fluorescence, Chemiluminescence and Visible Light Imaging program (Alpha Innotech, San Leandro, CA, USA). The expression of either the wt or mutant ZIP1-Myc protein was then normalized by the expression of GRP78.

Acknowledgements

This work was supported by the United States Department of Agriculture Grant: CRIS-5306-515-30-014-00D.

References

1 Palmiter RD & Findley SD (1995) Cloning and characterization of a mammalian zinc transporter that confers resistance to zinc. *EMBO J* **14**, 639–649.
2 Palmiter RD, Cole TB & Findley SD (1996) ZnT-2, a mammalian protein that confers resistance to zinc by facilitating vesicular sequestration. *EMBO J* **15**, 1784–1791.

3 Palmiter RD, Cole TB, Quaife CJ & Findley SD (1996) ZnT-3, a putative transporter of zinc into synaptic vesicles. *Proc Natl Acad Sci USA* **93**, 14934–14939.
4 Huang L & Gitschier J (1997) A novel gene involved in zinc transport is deficient in the lethal milk mouse. *Nat Genet* **17**, 292–297.
5 Inoue K, Matsuda K, Itoh M, Kawaguchi H, Tomoike H, Aoyagi T, Nagai R, Hori M, Nakamura Y & Tanaka T (2002) Osteopenia and male-specific sudden cardiac death in mice lacking a zinc transporter gene, Znt5. *Hum Mol Genet* **11**, 1775–1784.
6 Huang L, Kirschke CP & Gitschier J (2002) Functional characterization of a novel mammalian zinc transporter, ZnT6. *J Biol Chem* **277**, 26389–26395.
7 Kirschke CP & Huang L (2003) ZnT7, a novel mammalian zinc transporter, accumulates zinc in the golgi apparatus. *J Biol Chem* **278**, 4096–4102.
8 Chimienti F, Devergnas S, Favier A & Seve M (2004) Identification and cloning of a beta-cell-specific zinc transporter, ZnT-8, localized into insulin secretory granules. *Diabetes* **53**, 2330–2337.
9 Palmiter RD & Huang L (2004) Efflux and compartmentalization of zinc by members of the SLC30 family of solute carriers. *Pflugers Arch – Eur J Physiol* **447**, 744–751.
10 Gaither LA & Eide DJ (2001) The human ZIP1 transporter mediates zinc uptake in human K562 erythroleukemia cells. *J Biol Chem* **276**, 22258–22264.
11 Gaither LA & Eide DJ (2000) Functional expression of the human hZIP2 zinc transporter. *J Biol Chem* **275**, 5560–5564.
12 Kelleher SL & Lonnerdal B (2005) Zip3 plays a major role in zinc uptake into mammary epithelial cells and is regulated by prolactin. *Am J Physiol Cell Physiol* **288**, C1042–C1047.
13 Wang K, Zhou B, Kuo YM, Zemansky J & Gitschier J (2002) A novel member of a zinc transporter faily defective in acrodermatitis enteropathica. *Am J Hum Genet* **71**, 66–73.
14 Wang F, Kim BE, Petris MJ & Eide DJ (2004) The mammalian ZIP5 protein is a zinc transporter that localizes to the basolateral surface of polarized cells. *J Biol Chem* **279**, 51433–51441.
15 Taylor KM, Morgan HE, Johnson A, Hadley LJ & Nicholson RI (2003) Structure-function analysis of LIV-1, the breast cancer-associated protein that belongs to a new subfamily of zinc transporters. *Biochem J* **375**, 51–59.
16 Taylor KM, Morgan HE, Johnson A & Nicholson RI (2004) Structure-function analysis of HKE4, a member of the new LIV-1 subfamily of zinc transporters. *Biochem J* **377**, 131–139.
17 Huang L, Kirschke CP, Zhang Y & YuYY (2005) The ZIP7 gene (Slc39a7) encodes a zinc transporter involved in zinc homeostasis of the Golgi apparatus. *J Biol Chem* **280**, 15456–15463.
18 Eide DJ (2004) The SLC39 family of metal ion transporters. *Pflugers Arch – Eur J Physiol* **447**, 796–800.
19 Kambe T, Yamaguchi-Iwai Y, Sasaki R & Nagao M (2004) Overview of mammalian zinc transporters. *Cell Mol Life Sci* **61**, 49–68.
20 Andree KB, Kim J, Kirschke CP, Gregg JP, Paik H, Joung H, Woodhouse L, King JC & Huang L (2004) Investigation of lymphocyte gene expression for use as biomarkers for zinc status in humans. *J Nutr* **134**, 1716–1723.
21 Cousins RJ, Blanchard RK, Popp MP, Liu L & Cao J (2003) A global view of the selectivity of zinc deprivation and excess on genes expressed in human THP-1 mononuclear cells. *Proc Natl Acad Sci USA* **100**, 6952–6957.
22 Dufner-Beattie J, Wang F, Kuo YM, Gitschier J, Eide D & Andrews GK (2003) The acrodermatitis enteropathica gene ZIP4 encodes a tissue-specific, zinc-regulated zinc transporter in mice. *J Biol Chem* **278**, 33474–33481.
23 Liuzzi JP, Lichten LA, Rivera S, Blanchard RK, Aydemir TB, Knutson MD, Ganz T & Cousins RJ (2005) Interleukin-6 regulates the zinc transporter Zip14 in liver and contributes to the hypozincemia of the acute-phase response. *Proc Natl Acad Sci USA* **102**, 6843–6848.
24 Wang F, Dufner-Beattie J, Kim BE, Petris MJ, Andrews G & Eide DJ (2004) Zinc-stimulated endocytosis controls activity of the mouse ZIP1 and ZIP3 zinc uptake transporters. *J Biol Chem* **279**, 24631–24639.
25 Kim BE, Wang F, Dufner-Beattie J, Andrews GK, Eide DJ & Petris MJ (2004) Zn^{2+}-stimulated endocytosis of the mZIP4 zinc transporter regulates its location at the plasma membrane. *J Biol Chem* **279**, 4523–4530.
26 Gitan RS & Eide DJ (2000) Zinc-regulated ubiquitin conjugation signals endocytosis of the yeast ZRT1 zinc transporter. *Biochem J* **346**, 329–336.
27 Bonifacino JS & Traub LM (2003) Signals for sorting of transmembrane proteins to endosomes and lysosomes. *Annu Rev Biochem* **72**, 395–447.
28 Janvier K & Bonifacino JS (2005) Role of the endocytic machinery in the sorting of lysosome-associated membrane proteins. *Mol Biol Cell* **16**, 4231–4242.
29 Rapoport I, Chen YC, Cupers P, Shoelson SE & Kirchhausen T (1998) Dileucine-based sorting signals bind to the beta chain of AP-1 at a site distinct and regulated differently from the tyrosine-based motif-binding site. *EMBO J* **17**, 2148–2155.
30 McNiven M & Thompson HM (2006) Vesicle formation at the plasma membrane and trans-Golgi network: the same but different. *Science* **313**, 1591–1594.

31 Dell'Angelica E, Mullins C & Bonifacino JS (1999) AP-4, a novel protein complex related to clathrin adaptors. *J Biol Chem* **274**, 7278–7285.
32 Hirst J, Bright NA, Rous B & Robinson MS (1999) Characterization of a fourth adaptor-related protein complex. *Mol Biol Cell* **10**, 2787–2802.
33 Dufner-Beattie J, Kuo YM, Gitschier J & Andrews GK (2004) The adaptive response to dietary zinc in mice involves the differential cellular localization and zinc regulation of the zinc transporters ZIP4 and ZIP5. *J Biol Chem* **279**, 49082–49090.
34 Mellman I (1996) Endocytosis and molecular sorting. *Annu Rev Cell Dev Biol* **12**, 575–625.
35 Milon B, Dhermy D, Pountney D, Bourgeois M & Beaumont C (2001) Differential subcellular localization of hZip1 in adherent and non-adherent cells. *FEBS* **507**, 241–246.
36 Huang L, Kirschke CP & Zhang Y (2006) Decreased intracellular zinc in human tumorigenic prostate epithelial cells: a possible role in prostate cancer progression. *Cancer Cell Int* **6**, 10.
37 Nakamura N, Rabouille C, Watson R, Nilsson T, Hui N, Slusarewicz P, Kreis TE & Warren G (1995) Characterization of a cis-Golgi matrix protein, GM130. *J Cell Biol* **131**, 1715–1726.
38 Sheff D, Daro EA, Hull M & Mellman I (1999) The receptor recycling pathway contains two distinct populations of early endosomes with different sorting functions. *J Cell Biol* **145**, 123–139.
39 Dunn W, Connolly TP & Hubbard AL (1986) Receptor-mediated endocytosis of epidermal growth factor by rat hepatocytes: receptor pathway. *J Cell Biol* **102**, 24–36.
40 Tsacoumango A, Kil SJ, Ma L, Sönnichsen FD & Carlin C (2005) A novel dileucine lysosomal-sorting-signal mediates intracellular EGF-receptor retention independently of protein ubiquitylation. *J Cell Sci* **118**, 3959–3971.
41 Kil S & Carlin C (2000) EGF receptor residues Leu^{679}, Leu^{680} mediate selective sorting of ligand-receptor complexes in early endosomal compartments. *J Cell Physiol* **185**, 47–60.
42 Dikic I (2003) Mechanisms controlling EGF receptor endocytosis and degradation. *Biochem Soc Trans* **31**, 1178–1181.
43 Bouley R, Lin HY, Raychowdhury MK, Marshansky V, Brown D & Ausiello DA (2005) Downregulation of the vasopressin type 2 receptor after vasopressin-induced internalization: involvement of a lysosomal degradation pathway. *Am J Physiol Cell Physiol* **288**, C1390–C1401.
44 Zhao H & Eide D (1996) The yeast ZRT1 gene encodes the zinc transporter protein of a high-affinity uptake system induced by zinc limitation. *Proc Natl Acad Sci USA* **93**, 2454–2458.
45 Petris MJ & Mercer JF (1999) The Menkes protein (ATP7A; MNK) cycles via the plasma membrane both in basal and elevated extracellular copper using a C-terminal di-leucine endocytic signal. *Hum Mol Genet* **8**, 2107–2115.
46 Cobbold C, Ponnambalam S, Francis MJ & Monaco AP (2002) Novel membrane traffic steps regulate the exocytosis of the Menkes disease ATPase. *Hum Mol Genet* **11**, 2855–2866.
47 Pase L, Voskoboinik I, Greenough M & Camakaris J (2004) Copper stimulates trafficking of a distinct pool of the Menkes copper ATPase (ATP7A) to the plasma membrane and diverts it into a rapid recycling pool. *Biochem J* **378**, 1031–1037.
48 Lane C, Petris MJ, Benmerah A, Greenough M & Camakaris J (2004) Studies on endocytic mechanisms of the menkes copper-translocating P-type ATPase (ATP7A; MNK). Endocytosis of the menkes protein. *Biometals* **17**, 87–98.
49 Huang F, Jiang X & Sorkin A (2003) Tyrosine phosphorylation of the beta2 subunit of clathrin adaptor complex AP-2 reveals the role of a di-leucine motif in the epidermal growth factor receptor trafficking. *J Biol Chem* **278**, 43411–43417.
50 Koh YH, von Arnim CA, Hyman BT, Tanzi RE & Tesco G (2005) BACE is degraded via the lysosomal pathway. *J Biol Chem* **280**, 32499–32504.
51 Letourneur F & Klausner RD (1992) A novel di-leucine motif and a tyrosine-based motif independently mediate lysosomal targeting and endocytosis of CD3 chains. *Cell* **69**, 1143–1157.
52 Dietrich J, Hou X, Wegener AM & Geisler C (1994) CD3 gamma contains a phosphoserine-dependent di-leucine motif involved in down-regulation of the T cell receptor. *EMBO J* **13**, 2156–2166.